

A review of Mössbauer data on trioctahedral micas: Evidence for tetrahedral Fe³⁺ and cation ordering

M. DARBY DYAR*

Division of Geological and Planetary Sciences, California Institute of Technology, Pasadena, California 91125, U.S.A.

ABSTRACT

Over fifty studies on Mössbauer spectroscopy of trioctahedral micas are summarized and reviewed in order to determine reasonable ranges for parameters of different Fe sites. Typical values (in units of mm/s) include Fe_{M2}²⁺—isomer shift (δ) = 1.13, quadrupole splitting (Δ) = 2.58; Fe_{M1}²⁺— δ = 1.12 and 1.16, Δ = 2.05 and 2.75; Fe_{M1}³⁺— δ = 0.40, Δ = 0.55; Fe_{M2}³⁺— δ = 0.40, Δ = 1.00; Fe_{tet}²⁺— δ = 0.20, Δ = 0.50. The effects of major-element composition on Mössbauer parameters are assessed and found to be minimal, though the substitution of Li in the octahedral sheet systematically affects the quadrupole splitting of the Fe_{M1}²⁺ doublet. The Mössbauer and compositional data considered together show that tetrahedral Al \leftrightarrow Fe³⁺ substitution may be controlled by octahedral cation size and that M2-M1 cation ordering is ubiquitous.

INTRODUCTION

When the technique of Mössbauer spectroscopy was initially applied to minerals, biotites were among the first samples to be analyzed (Pollak et al., 1962). Since then a large number of trioctahedral micas have been studied with the Mössbauer effect. This paper evaluates only the room-temperature work done over the past 23 years, as the effects of temperature and dehydroxylation on Mössbauer studies of micas have been reviewed by Heller-Kallai and Rozenson (1981). Three distinct areas of investigation are addressed: (1) What are reasonable ranges for Mössbauer parameters of Fe in the different sites in micas? (2) How do variables such as composition affect Mössbauer results? Are isomer shift (I.S. or δ) and quadrupole splitting (Q.S. or Δ) affected by other cations adjacent to Fe in the mica structure? Is there a difference in peak-area data of igneous vs. metamorphic samples? (3) Is there evidence for cation ordering in micas?

Figure 1 shows a drawing of the mica structure that can be used in the following discussion: details of structural variations in trioctahedral micas are given by Bailey (1984a, 1984b), Guggenheim (1984), and Weiss et al. (1985).

RANGES OF MÖSSBAUER PARAMETERS

Mössbauer and electron-microprobe data on trioctahedral micas are compiled in the Appendix and plotted in Figure 2. For Fe in oxygen environments, the isomer shift and quadrupole-splitting values (as calibrated in millimeters per second relative to an Fe-foil spectrum) most commonly fall in the following ranges (Dyar, 1984): Fe_{tet}³⁺— δ = 0.15–0.30, Δ = 0.30–0.60; Fe_{oct}³⁺— δ = 0.35–

0.50, Δ = 0.40–1.0; Fe_{tet}²⁺— δ = 0.90–1.0, Δ = 1.5–1.8; Fe_{oct}²⁺— δ = 1.1–1.2, Δ = 1.8–3.1.

Figure 2 shows a plot of isomer shift vs. quadrupole splitting for all the analyses collected. The data for Fe²⁺ at M2 cluster tightly around Δ = 2.58 and δ = 1.13 mm/s, suggesting that the local geometry about the M2 site is not radically affected by the broad compositional range of these samples. For the data for Fe²⁺ at M1, one group of analyses clusters around Δ = 2.05 and δ = 1.12, and a second, more scattered group falls around Δ = 2.75 and δ = 1.16 mm/s. For Fe²⁺, lower quadrupole splitting generally implies more distortion around a site (the reverse is true for Fe³⁺), owing to some combination of the effects of metal-to-oxygen distances and angular components (however, this relationship has never been fully quantified). Therefore there seem to be three types of Fe²⁺ sites: a distorted Fe²⁺ M1 site, the Fe²⁺ M2 site, and a regular Fe²⁺ M1 site.

Mössbauer data for Fe³⁺ sites are less well defined; however, in my opinion the wider range of values may be due to a problem with the fitting procedures and is *not* dependent on compositional effects. Fe³⁺ at M2 and M1 has a similar range of δ = 0.35–0.65 mm/s, although each group has its own range of Δ = 0.11–0.80 and 0.57–1.24 mm/s respectively. Fe³⁺ peaks are almost always less intense than the corresponding Fe²⁺ peaks in the same samples (except in ferri-annites and ferri-phlogopites). In general, fitted Mössbauer doublets are less precise when peak areas are small. The samples in which Fe³⁺ Δ values lie between 0.60 and 1.0 mm/s probably represent spectra in which Fe³⁺ was present at both M2 and M1, but in such small quantities that it was impossible to distinguish them. The resultant single Fe³⁺ doublet in such samples has a Δ that is the average of the Δ values for the two separate sites.

* Present address: Department of Geology, University of Oregon, Eugene, Oregon 97403, U.S.A.

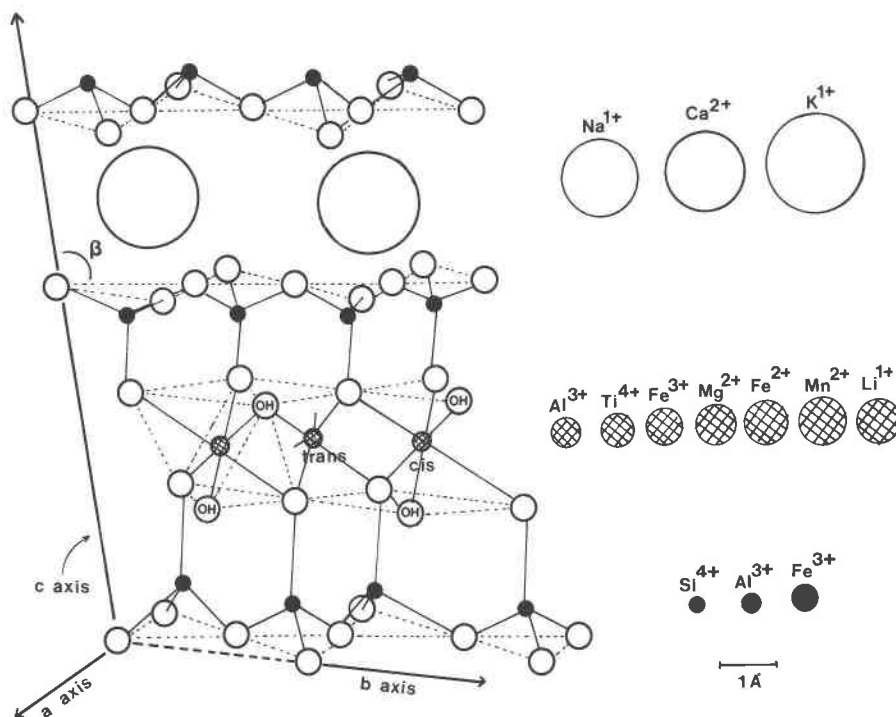


Fig. 1. Scale drawing of a typical trioctahedral mica crystal structure. Ions in the structure are shown schematically; relative (to scale) sizes of the various substituting cations are shown at right.

In the petrologic literature, there has been a consensus that Fe^{3+} does not occur at tetrahedral sites in biotites (Guidotti, 1984), although a few authors have made a case for $\text{Fe}_{\text{tet}}^{3+}$ when $\Sigma(\text{Si} + \text{Al}) < 8$ (Foster, 1960; Dawson and Smith, 1977; Delaney et al., 1980; Miyano and Miyano, 1982). However, Mössbauer parameters for tetrahedral Fe^{3+} are well-defined by studies of tetra-ferri-phlogopite (see sample 87) and clintonites (samples 59–63). Of the Mössbauer data collected in this study, 31 samples contain $\text{Fe}_{\text{tet}}^{3+}$ with parameters averaging $\delta = 0.20$ and $\Delta = 0.50$ mm/s. Twenty samples are Al-deficient, whereas 11 have excess Al. This observation will be discussed in a later section.

INTERVALENCE CHARGE TRANSFER AND MÖSSBAUER SPECTRA OF BIOTITES

It is well known from optical spectra that charge transfer of electrons can occur between Fe^{2+} and Fe^{3+} in edge-sharing octahedra (Gilkes et al., 1972; Robbins and Strens, 1972; Smith, 1978); biotites are pleochroic because of this intervalence phenomena. However, intervalence charge-transfer doublets do not appear in biotite spectra as they do in ilvaite, magnetite, and many other minerals (Burns, 1981). This issue can be addressed with a brief explanation of the difference between the two types of mixed valence interactions (Nolet and Burns, 1979). The term “charge transfer” is normally applied to dynamic optical (phonon) transitions, as have been observed by the workers listed above. Electron delocalization refers to thermally activated phenomena as observed in a Möss-

bauer spectrum. In the case of biotite, the optical transition is easily observed, but the thermal interaction is not observed at room temperature. Possibly the charge transfer in biotite is occurring too rapidly to be measured by the Mössbauer effect.

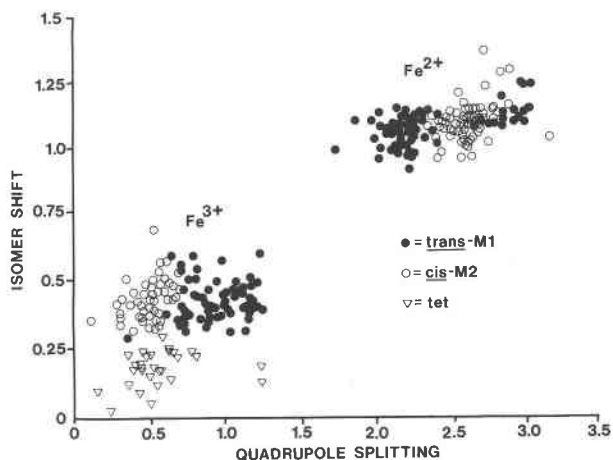


Fig. 2. Plot of isomer shift vs. quadrupole splitting (in mm/s) for all analyses collected (see Appendix). Following the precedent of Bancroft and Brown (1975), the Fe^{3+} doublet with the largest quadrupole splitting is assigned to represent the *trans*-M1 site; the Fe^{3+} doublet with the smaller Δ corresponds to the *cis*-M2 site. For Fe^{2+} , the correspondence is reversed: small Δ is equated to the *trans*-M1 site, and large Δ represents the *cis*-M2 site.

Table 1. Correlation coefficients (*r*) for Mössbauer and compositional parameters regressed against one another

Al _{iv}	Fe _v ³⁺	Al _{vi}	Ti	Fe _{vi} ³⁺	Mg	Fe _{vi} ²⁺	Mn	Li	Ca	Na	K	δ1
-0.97	0.04	-0.15	-0.32	0.06	-0.20	0.13	0.11	0.49	-0.88	0.09	0.81	0.25
	-0.27	0.20	0.34	-0.05	0.18	-0.15	-0.14	-0.46	0.82	-0.06	-0.75	-0.21
		-0.22	-0.26	-0.04	0.01	0.17	0.00	-0.23	0.08	-0.12	-0.11	-0.05
			0.03	-0.20	-0.43	-0.02	0.04	0.77	0.23	-0.26	0.00	0.26
				0.38	-0.38	0.25	-0.13	-0.54	0.20	-0.15	-0.01	-0.25
					-0.40	0.36	-0.09	-0.04	-0.20	-0.13	0.11	-0.23
						-0.74	0.01	-0.71	0.29	0.30	-0.30	0.00
							-0.29	-0.44	-0.41	-0.30	0.36	-0.07
								0.77	-0.14	0.18	-0.08	0.04
									-0.43	-0.61	-0.09	0.31
										-0.10	-0.96	-0.38
											0.05	0.21
												0.26

EFFECTS OF MICA COMPOSITION ON MÖSSBAUER PARAMETERS

Heller-Kallai and Rozenson (1981) listed six factors that could affect Mössbauer parameters of Fe at the octahedral sites in phyllosilicates: (1) nature of the octahedral sheets, (2) Fe content of the samples, (3) chemical composition of the octahedral sheets, (4) nature and distribution of next-nearest neighbors, (5) geometry of the sites, and (6) covalency effects.

To investigate possible relationships between composition and Mössbauer parameters, a multiple linear correlation analysis was done on the data in the Appendix. Multiple correlation coefficients (*R*) were computed for each pair of variables and are listed in Table 1. In addition to analysis of each single variable against every other single variable, correlation coefficients were also calculated for combinations of up to three variables against all other possible combinations (of up to three variables); 8 235 711 combinations were checked.

A few obvious correlations exist; for example, tetrahedral Si and Al have a high correlation (*R* = 0.97) because they often fill the site. Similarly Ca and K (*R* = -0.96) correlate highly. Cations that commonly substitute for each other are strongly related; octahedral Fe²⁺ and Mg have an *R* = -0.74.

As mentioned above, the fact that Fe_{M1}²⁺ Δ values cluster in two groups might be attributed to some compositional effect. Analysis of multiple combinations of variables clearly identifies the source of this effect; regression of Δ of Fe_{M1}²⁺ vs. octahedral Al + Fe³⁺ + Li yields *R* = 0.95. The Δ of Fe_{M1}²⁺ vs. Li content alone is also strongly correlated (*R* = 0.87), though Δ of Fe_{M1}²⁺ vs. Al_{vi} + Fe_{vi}³⁺ is not (*R* less than 0.70). Possibly the presence of the rela-

tively large Li cation (charge-balanced by Al and Fe³⁺) in the octahedral layer is accommodated by structural rearrangement or distortion of adjacent oxygens, which is in turn reflected by increased Δ values for Fe²⁺ at M1. Recent work by Weiss et al. (1985) indicates that M1 tends to be most distorted by flattening in those ordered cases where it is occupied by a large cation (such as Li); this argument supports the observed increase in Δ for Li-bearing samples. Unfortunately, Li analyses could be found in the literature for only 19 samples in the data base; perhaps the correlation would be even stronger if more Li data were available.

SITE-OCCUPANCY DATA APPLIED TO CRYSTAL CHEMISTRY

Perhaps the most useful aspect of this literature review is that it has yielded a unique set of data on Fe site occupancy for trioctahedral micas. Before exploring the relationships of this complete data set, it is important to add a few cautionary notes on the reliability of site-occupancy data generated by fitting of Mössbauer spectra. Preliminary work on the precision of the Mössbauer technique in simple spectra (as calculated from repeated runs of the same sample) suggests that area data are good to ±3% of the total area. This represents a lower limit on the technique. Furthermore, there is often a problem with preferred orientation of the samples, which is difficult to overcome in micas. Hogg and Meads (1970) suggested that this is not a problem if the particle size in the sample holder is below 5 μm. Careful sample preparation, including mounting the particles with some inert medium to prevent their becoming oriented, is always called for in mica studies. However, in a survey paper such as this,

Table 1. *Continued*

$\Delta 1$	$\delta 2$	$\Delta 2$	$\delta 3$	$\Delta 3$	$\delta 4$	$\Delta 4$	$\delta 5$	$\Delta 5$	% Fe ²⁺	M2/M1	
0.41	0.20	0.46	-0.04	-0.13	-0.61	-0.52	-0.27	-0.32	0.32	-0.20	Si
-0.37	-0.24	-0.45	0.10	0.13	0.75	0.63	0.26	0.28	-0.19	0.18	Al _{iv}
0.01	0.16	0.14	-0.24	-0.03	-0.65	-0.55	-0.05	0.04	-0.37	0.03	Fe _v ³⁺
-0.31	0.18	0.29	-0.30	-0.18	0.14	0.25	-0.02	0.12	0.19	0.14	Al _{iv}
-0.32	-0.49	-0.51	0.15	-0.24	0.23	0.08	-0.59	0.09	0.09	-0.22	Ti
-0.01	-0.26	-0.30	-0.06	-0.03	0.07	-0.08	-0.04	-0.24	-0.11	0.00	Fe _v ³⁺
0.18	0.20	0.21	0.46	0.25	0.01	0.25	0.38	0.21	-0.23	-0.14	Mg
-0.09	-0.18	-0.25	-0.25	-0.35	-0.28	-0.59	-0.45	-0.16	0.27	-0.04	Fe _v ²⁺
-0.09	-0.28	-0.27	-0.32	0.08	0.27	0.15	0.32	0.09	-0.59	-0.07	Mn
-0.05	0.66	0.87	-0.59	0.29	—	—	—	—	0.24	0.69	Li
-0.40	-0.23	-0.36	0.08	0.25	-0.08	0.11	0.50	0.30	-0.48	0.32	Ca
0.38	0.38	0.27	0.10	0.25	0.43	0.36	0.19	0.12	-0.02	0.07	Na
0.28	0.17	0.32	-0.08	-0.30	0.27	0.20	-0.40	-0.23	0.42	-0.39	K
0.36	0.80	0.40	0.14	-0.03	-0.06	0.06	-0.25	0.32	0.30	0.15	$\delta 1$
	0.35	0.30	0.13	0.29	-0.02	-0.19	0.07	-0.19	0.08	-0.07	$\Delta 1$
		0.58	0.15	0.09	-0.16	-0.05	0.09	0.08	0.22	0.15	$\delta 2$
			-0.12	0.01	-0.51	-0.25	0.07	-0.32	0.19	-0.07	$\Delta 2$
				-0.16	0.34	0.34	-0.33	0.17	0.14	-0.27	$\delta 3$
					0.47	0.28	0.72	0.52	-0.25	0.51	$\Delta 3$
						0.53	-0.92	-0.68	0.26	0.08	$\delta 4$
							-0.72	-0.89	0.14	-0.20	$\Delta 4$
								0.22	-0.22	0.21	$\delta 5$
									-0.04	0.53	$\Delta 5$
										-0.17	% Fe ²⁺

it is impossible to determine if anomalous area data are the result of faulty sample preparation.

Another problem with Mössbauer area data hinges on the undetermined value for relative recoil-free fraction in micas. In some minerals, such as garnets, the line strength of Fe³⁺ peaks can be significantly larger than those of Fe²⁺ peaks (Whipple, 1974). In the garnet structure, the Fe³⁺ is held more rigidly at its octahedral site, such that fewer of the Fe³⁺ atoms recoil than do Fe²⁺ at their eight-coordinated sites. The resultant Mössbauer spectrum appears to have more Fe³⁺ than is actually present, and the resultant area data must be corrected for this differential recoil-free fraction effect. Whipple (1974) examined a phlogopite and a biotite to determine relative line strengths, but unfortunately his results were inconclusive (R_{biotite} was 1.18, $R_{\text{phlogopite}}$ was 0.78, where R = Mössbauer-determined Fe³⁺/Fe²⁺ ratio divided by the chemically determined Fe³⁺/Fe²⁺ ratio). Thus it is not known whether differential recoil-free fraction effects are biasing the Mössbauer area data; it is hoped that such effects would be small.

Finally, another problem with the area data for biotites was raised by Mineeva (1978), who interpreted the wide spread of M2/M1 values to be a sign of overfitting; she concluded that only two doublets were present. In my opinion, the area data *are* real, for the following reasons: (1) peak *positions* for the M2 and M1 (both Fe³⁺ and Fe²⁺) peaks are fairly consistent throughout the 151 samples reviewed here. If two doublets do not really exist, the positions of all the peaks would be more random. (2) As discussed above, Δ values for the Fe_{M1}³⁺ doublet can be explained as a systematic function of octahedral Li, Al, and Fe³⁺ content. If the M1 doublet does not really exist,

it is unlikely that such a logical correlation would be found between those variables.

STRUCTURAL CHANGES BASED ON CATION SIZE

The compositional substitutions in mica are firmly based on the principle of maintenance of *charge balance* in the structure. However, as was discussed in the Introduction, the sizes of substituting cations also affect the structure. Hazen and Wones (1972) found a strong correlation between ionic radius of R²⁺ and b_m , which is intuitively obvious when the wide range of cation sizes is considered (see Fig. 1). Tetrahedral rotation may also accommodate size differences between tetrahedral and octahedral sheets. It is known that α is minimized when octahedral-cation radius increases to 0.76 Å (Hazen and Wones, 1972); it is also known that α may be as large as 22° in clintonites, in which the low Si/Al_{tet} ratio compensates for Ca substitution at the A site (Annersten and Olesch, 1978). Data assembled for this review provide yet another important constraint on Si/Al_{tet} as a function of cation size, as follows:

It was noticed that in 11 of the 31 Fe_{tet}³⁺-bearing samples, Si + Al ≥ 8. Tetrahedral Al is apparently displaced by Fe³⁺. This does not comply with crystal-chemical expectations; the small Al cation generally should have a greater preference for the smaller tetrahedral site than does the larger Fe_{tet}³⁺. Contrary to the results of Annersten and Olesch (1978), Figure 3 shows that Si/Al ratios do not particularly *control* this substitutional phenomenon: triangles representing Fe_{tet}³⁺-bearing samples with Si + Al ≥ 8 are intermixed with the circles for Al-deficient (Si + Al ≤ 8) Fe³⁺ samples (except for the clintonite data,

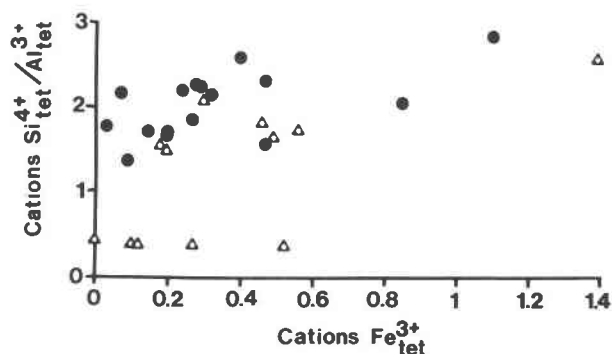


Fig. 3. Si/Al ratio vs. $\text{Fe}_{\text{tet}}^{3+}$ cations for samples where $\text{Fe}_{\text{tet}}^{3+} > 0$. Triangles represent data for samples where $\text{Si} + \text{Al} \geq 8$, and circles represent Al-deficient micas. The five lowest triangles are clintonite data from Annersten and Olesch (1974).

which have $\text{Si}/\text{Al} < 1$). If Si/Al ratio does not control $\text{Fe}_{\text{tet}}^{3+}$ in non-Al-deficient samples, what does?

Annersten and Olesch (1978) postulated that the effect of Ca in the interlayer sites was to increase the relative size of the tetrahedra, making it possible for the larger Fe^{3+} cation to enter. As Figure 4 shows, the size of the A site cations does not seem to correlate with $\text{Fe}_{\text{tet}}^{3+}$ displacing Al. However, Figure 5 demonstrates that the phenomenon does occur when the average size of the octahedral cations is low ($< 0.68 \text{ \AA}$), implying an abundance of 3+ and 4+ cations in the octahedral sheet. Perhaps small cation size can be correlated with the presence of octahedral *vacancies* (needed to charge-balance the smaller, highly charged cations) that would increase the size of the octahedral sheet and necessitate enlargement of the

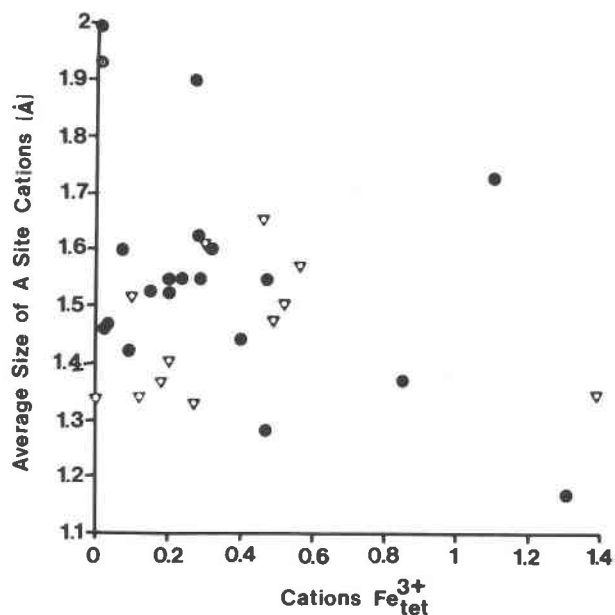


Fig. 4. Average size of the A-site interlayer cations vs. $\text{Fe}_{\text{tet}}^{3+}$ content, with triangles representing samples with $\text{Si} + \text{Al} > 8$. There is no apparent division between triangles and circles (Al-deficient micas).

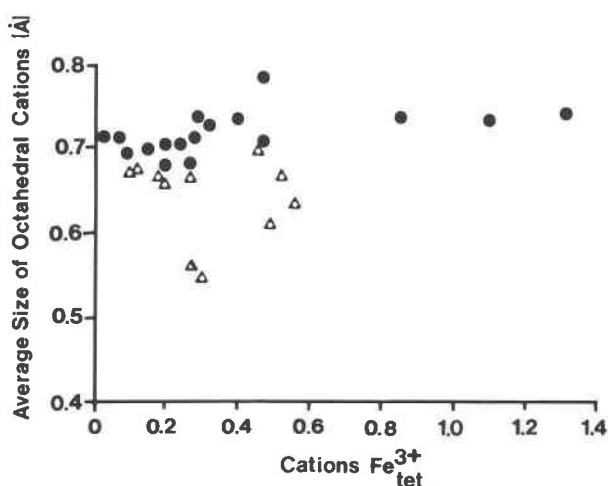


Fig. 5. Average size of the octahedral cations vs. $\text{Fe}_{\text{tet}}^{3+}$ content. Triangles represent samples where $\text{Si} + \text{Al} > 8$. Note that when octahedral-cation size is less than $\sim 0.68 \text{ \AA}$, Fe^{3+} substitutes at the tetrahedral position regardless of how much Al is present.

tetrahedra to allow a fit between layers. Enlarged tetrahedra could then easily accommodate Fe^{3+} cations.

CATION ORDERING

Crystal-structure refinement is the standard method for examination of cation ordering in micas; literature data are summarized in Bailey (1984a). He showed that tetrahedral cation ordering does occur (albeit infrequently) in micas.

On the other hand, octahedral cation ordering is more common. Although early studies found little or no evidence for significant ordering of Mg and Fe in micas (Goodman and Wilson, 1973; Hazen and Burnham, 1973), subsequent workers have suggested that Fe^{2+} prefers M2 (Annersten, 1975), or M1 (Levillain et al., 1981), and that Fe^{2+} in low-grade metamorphic biotites is ordered at M2 (Heller-Kallai and Rozenson, 1981) or M1 (Annersten, 1974). Ohta et al. (1982) postulated that partial cation ordering of Fe^{3+} at M2 may occur, but Fe^{2+} is randomly distributed over the two M2 and one M1 sites in each unit cell.

The Mössbauer effect is of limited use in deciphering site occupancies in micas because it can only describe the location of Fe cations in the structure. The data collected in this study demonstrate that the ratio of Fe cations in the *cis*-M2 : *trans*-M1 sites is rarely 2:1. This suggests that some cation ordering is occurring in the octahedral sheet. It is tempting to assume that only Fe and Mg are ordering; such an assumption would allow development of an equilibrium constant for Fe-Mg exchange at the two sites. However, it is impossible to determine from Mössbauer data alone which of the many cations in the octahedral sheets is ordering (especially in micas with such varied compositions and parageneses).

As can be seen in Table 1, the amount of Fe^{2+} ordering

is not correlated with any of the single compositional variables listed, including $\text{Fe}^{2+}/\Sigma\text{Fe}$. An attempt was made to correlate $\text{Fe}_{\text{M2}}^{2+}/\text{Fe}_{\text{M1}}^{2+}$ ratios with parageneses listed in Appendix Table 4; however there is not enough detailed information to make a worthwhile comparison. A more dedicated study of sample paragenesis vs. ordering of cations among M2 and M1 sites, using a large number of compositionally similar (and simpler) samples, is in progress to determine the systematics of cation-ordering processes. In the context of this literature review, it can only be said that the ratio of Fe^{2+} at the M2 and M1 sites is highly variable (from 0.70 to 5.14) and does not seem to be a simple function of any single compositional variable, including $\text{Fe}^{2+}/\Sigma\text{Fe}$.

SUMMARY

This review of Mössbauer studies of trioctahedral micas has three principal conclusions:

1. Typical values for Mössbauer parameters of different mica sites are as follows: $\text{Fe}_{\text{M2}}^{2+} - \delta = 1.13$, $\Delta = 2.58$ mm/s; $\text{Fe}_{\text{M1}}^{2+} - \delta = 1.12$ and 1.16 , $\Delta = 2.05$ and 2.75 mm/s; $\text{Fe}_{\text{M1}}^{3+} - \delta = 0.40$, $\Delta = 0.55$ mm/s; $\text{Fe}_{\text{M2}}^{3+} - \delta = 0.40$, $\Delta = 1.00$ mm/s; $\text{Fe}_{\text{tet}}^{3+} - \delta = 0.20$, $\Delta = 0.50$ mm/s. It is also noteworthy that no Mössbauer evidence for a doublet representing intervalence $\text{Fe}^{3+} \rightarrow \text{Fe}^{2+}$, delocalized species has been found.

2. The effects of composition on Mössbauer parameters seem to be minimal, although the addition of Li to the octahedral sheet systematically affects quadrupole splitting of the $\text{Fe}_{\text{M1}}^{3+}$ doublet.

3. The addition of the Mössbauer site-occupancy data to compositional information shows that tetrahedral Al \leftrightarrow Fe^{3+} substitution may be controlled by octahedral cation size and that M2-M1 cation ordering is ubiquitous.

ACKNOWLEDGMENTS

The author thanks Roger Burns and George Rossman (and grants NSG-7601 and EAR-8212540, respectively) for support over different periods of this study. Scott Phillips is also gratefully acknowledged for statistical advice and the multiple regression program, SEARCH. Thorough reviews by Frank Hawthorne, S. W. Bailey, and an anonymous reviewer contributed greatly to the final version of this paper.

REFERENCES

Amirkhanov, Kh.I., Anokhina, L.K., Sardarov, S.S., Murina, G.A., and Gabitova, R.U. (1980) Absolute age of Aldan and Slyudyanka (USSR) biotites and phlogopites. In L.N. Ovchinnikov, Ed. *Vost Sib Dal'nego Vostoka*, p. 63–65. Izd Nauka, Moscow.

Annersten, H. (1974) Mössbauer studies of natural biotites. *American Mineralogist*, 59, 143–151.

——— (1975) Mössbauer study of iron in natural and synthetic biotites. *Fortschritte der Mineralogie*, 52, 583–590.

Annersten, H., and Olesch, M. (1978) Distribution of ferrous and ferric iron in clintonite and the Mössbauer characteristics of ferric iron in tetrahedral coordination. *Canadian Mineralogist*, 16, 199–203.

Annersten, H., Devanarganan, S., Haggstrom, L., and Wappling, R. (1971) Mössbauer study of synthetic ferri-phlogopite $\text{KMg}_3\text{Fe}^{3+}\text{Si}_3\text{O}_{10}(\text{OH})_2$. *Physica Status Solidi*, B48, K137–K138.

Astakhov, A.V., Voitkovskii, Y.B., Genralov, O.N., and Sidorov, S.V. (1975) NGR investigation of some lamellar and boron-containing silicates. *Kristallografiya*, 20, 769–774.

Bagin, V.I., Gendler, T.S., Dainyak, L.G., and Kuzmin, R.N. (1980) Mössbauer, thermomagnetic and X-ray study of cation ordering and high temperature decomposition in biotite. *Clays and Clay Minerals*, 28, 188–196.

Bailey, S.W. (1984a) Crystal chemistry of the true micas. *Mineralogical Society of America Reviews in Mineralogy*, 13, 13–60.

——— (1984b) Review of cation ordering in micas. *Clays and Clay Minerals*, 32, 81–92.

Bancroft, G.M., and Brown, J.R. (1975) A Mössbauer study of coexisting hornblends and biotites: Quantitative $\text{Fe}^{3+}/\text{Fe}^{2+}$ ratios. *American Mineralogist*, 60, 265–272.

Bancroft, G.M., Sham, T.K., Riddle, C., Smith, T.E., and Turek, A. (1977) Ferric/ferrous-iron ratios in bulk rock samples by Mössbauer spectroscopy: The determination of standard rock samples G2, GA, W1, and mica Fe. *Chemical Geology*, 19, 277–284.

Bowen, L.H., Weed, S.B., and Stevens, J.G. (1969) Mössbauer study of micas and their potassium-depleted products. *American Mineralogist*, 54, 72–84.

Burns, R.G. (1981) Intervalence transitions in mixed-valence minerals of iron and titanium. *Annual Reviews of Earth and Planetary Science*, 9, 354–377.

Chandra, Ramesh, and Lokanathan, S. (1977) Electric field gradient in biotite mica. *Physica Status Solidi*, b, 83, 273–280.

Chandra, Usha, and Lokanathan, S. (1982) A Mössbauer study of the effect of heat treatment on biotite micas. *Journal of Physics D: Applied Physics*, 15, 2331–2340.

Dawson, J.B., and Smith, J.V. (1977) The MARID (mica-amphibole-rutile-ilmenite-diopside) suite of xenoliths in kimberlites. *Geochimica et Cosmochimica Acta*, 41, 309–323.

Delaney, J.S., Smith, J.V., Carswell, D.A., and Dawson, J.B. (1980) Chemistry of micas from kimberlites and xenoliths. II. Primary- and secondary-textured micas from periodotite xenoliths. *Geochimica et Cosmochimica Acta*, 44, 857–872.

Dodge, F.C.W., Smith, V.C., and Mays, R.E. (1969) Biotites from granitic rocks of the central Sierra Nevada batholith, California. *Journal of Petrology*, 10, part 2, 250–271.

Drago, V., Baggio-Saitovitch, E., and Danon, J. (1977) Mössbauer spectroscopy of electron-irradiated natural layered silicates. *Journal of Inorganic and Nuclear Chemistry*, 39, 973–979.

Dyar, M.D. (1984) Precision and interlaboratory reproducibility of measurements of the Mössbauer effect in minerals. *American Mineralogist*, 69, 1127–1144.

Ericsson, T., Wappling, R., and Punakivi, K. (1977) Mössbauer spectroscopy applied to clay and related minerals. *Geologiska Foreningens I Stockholm Forhandlingar*, 99, 229–245.

Foster, M.D. (1960) Interpretation of the composition of trioctahedral micas. U.S. Geological Survey Professional Paper 354-B.

Gendler, T.S., Daynyak, L.G., and Kuzmin, R.N. (1978) Parameters of the Mössbauer spectrum of Fe^{3+} ions in biotite and continuity of biotite-oxybiotite transition at 300–900 K. *Geochemistry International*, 15, 17–22.

Gettys, W.L., and Stevens, J.G. (1981) Debye model calculation of second order Doppler shifts. In J.W. Robinson, Ed. *Handbook of spectroscopy III*, p. 496. CRC, Boca Raton, Florida.

Gilkes, R.J., Young, R.C., and Quirk, J.P. (1972) The oxidation of octahedral iron in biotite. *Clays and Clay Minerals*, 20, 303–315.

Goncharov, G.N., Moskvina, L.N., and Tomilov, S.B. (1971) Use of nuclear physical methods for studying the principles of the metasomatic substitution of siderophyllite. *Prikl Yad Spektrosk*, no. 2, 62–67.

Goodman, B.A., and Wilson, M.J. (1973) A study of the weathering of biotite using the Mössbauer effect. *Mineralogical Magazine*, 39, 448–454.

- Guggenheim, Stephen. (1984) The brittle micas. *Mineralogical Society of America Reviews in Mineralogy*, 13, 61–104.
- Guidotti, C.V. (1984) Micas in metamorphic rocks. *Mineralogical Society of America Reviews in Mineralogy*, 13, 357–467.
- Haggstrom, L., Wappling, R., and Annersten, H. (1969a) Mössbauer study of iron-rich biotites. *Chemical Physics Letters*, 4, 107–108.
- (1969b) Mössbauer study of oxidized iron silicate minerals. *Physica Status Solidi*, 33, 741–748.
- Hazen, R.W., and Wones, D.R. (1972) The effect of cation substitutions on the physical properties of trioctahedral micas. *American Mineralogist*, 57, 103–129.
- Heller-Kallai, L., and Rozenson, I. (1981) The use of Mössbauer spectroscopy of iron in clay mineralogy. *Physics and Chemistry of Minerals*, 7, 223–238.
- Hogarth, D.D., Brown, F.F., and Pritchard, A.M. (1970) Biabsorption, Mössbauer spectra, and chemical investigation of five phlogopite samples from Quebec. *Canadian Mineralogist*, 10, 710–722.
- Hogg, C.S., and Meads, R.E. (1970) The Mössbauer spectra of several micas and related minerals. *Mineralogical Magazine*, 37, 606–614.
- (1975) A Mössbauer study of thermal decomposition of biotites. *Mineralogical Magazine*, 40, 79–88.
- Huggins, F.E. (1976) Mössbauer studies of iron minerals under pressures of up to 200 kbars. In R.G.J. Strens, Ed. *The physics and chemistry of minerals and rocks*, p. 613–640. Wiley, New York.
- Ishida, K., and Hirowatari, F. (1980) On the chemical composition and Mössbauer spectra of manganoan phlogopite with reverse pleochroism. *Kobutsugaku Zasshi*, 14 (Tokubet sugo 3), 54–61.
- Ivanitskiy, V.P., Kalmechenko, A.M., Matyash, I.V., and Ihan'yak, T.P. (1975a) Mössbauer and PMR studies of oxidation and dehydroxylation in biotite. *Geokhimiya*, no. 12, 1864–1871.
- Ivanitskiy, V.P., Matyash, I.V., and Rakovich, F.I. (1975b) Effects of irradiation on the Mössbauer spectra of biotites. *Geochemistry International*, 12, 151–157, from *Geokhimiya*, no. 6, 850–856.
- (1975c) Mössbauer spectra of iron in biotite near ore as a prospecting criterion for radioactive elements (in Russian). *Dopovidi Akademii Nauk Ukrain's'koi RSR*, ser. B, no. 3, 206–209.
- Ivanitskiy, V.P., Kalinichenko, A.M., Matyash, I.V., Kudelya, V.K., Zayats, A.P., and Shvets, D.I. (1977) On the influence of gamma-radiation upon processes of oxidation, dehydroxylation and magnetic properties of some aluminosilicates (in Russian). *Geokhimiya*, no. 8, 237–245.
- Ivanitskiy, V.P., Kalinichenko, A.M., Matyash, I.V., Shvets, D.I., and Batiievskii, B.A. (1978) Distribution of octahedral cations as an index of the radiation stability of biotites (in Russian). *Konstitutsiya i Svoistva Mineralov*, 12, 47–54.
- Kohno, T., and Kakitani, S. (1972) Weathering alteration and the variation of Mössbauer spectra for biotites (in Japanese). *Zobutsugaku Zasshi*, 10, 499–506.
- Lefelhocz, J.F., Friedel, R.A., and Kohman, T.P. (1967) Mössbauer spectroscopy of iron in coal. *Geochimica et Cosmochimica Acta*, 31, 2261–2273.
- Levillain, Christian, Maurel, Pierre, and Menil, Francis. (1977) Localisation du fer, par voie chimique et par spectrométrie Mössbauer, dans la lepidolite du granite de Beavoir (Massif central français). *Bulletin de la Société Française de Minéralogie et de Cristallographie*, 100, 137–142.
- (1981) Mössbauer studies of synthetic and natural micas on the polyolithiorite-siderophyllite join. *Physics and Chemistry of Minerals*, 7, 71–76.
- Manapov, R.A., and Krinari, G.A. (1976) Gamma-resonance spectroscopy of layer silicates and some problems of their crystal chemistry. In Vinokurov, V.M., Ed. *Fiz Svoistva Miner Gorn Porod*, p. 110–122. Izdanja Kazan Universiteta, Kazan.
- Manapov, R.A., and Sitdikov, B.S. (1974) Mössbauer spectroscopic study of biotites of metamorphic rocks of the Tatar Arch Precambrian basement. *Geochemistry International*, 11, 976–980.
- Marfunin, A.S., Mkrtychyan, A.R., Nadzharyan, G.N., Nyussik, YaM., and Platonov, A.N. (1971) Optical and Mössbauer spectra of iron in some layered silicates (in Russian). *Izvestiya Akademii Nauk Azerbaidzhanskoi SSR, Seriya Geologo-Geograficheskikh*, 7, 87–93.
- Mineeva, R.M. (1978) Relationship between Mössbauer spectra and defect structure in biotites from electric field gradient calculations. *Physics and Chemistry of Minerals*, 2, 267–277.
- Miyano, T., and Miyano, S. (1982) Ferri-annite from the Dales Gorge Member iron-formations, Wittenoon area, Western Australia. *American Mineralogist*, 67, 1179–1194.
- Nolet, D.A., and Burns, R.G. (1979) Ilvaite: A study of temperature dependent electron delocalization by the Mössbauer effect. *Physics and Chemistry of Minerals*, 4, 221–234.
- Ohta, T., Takeda, H., and Takéuchi, Y. (1982) Mica polymorphism: Similarities in the crystal structures of coexisting 1M and 2M₁ oxybiotite. *American Mineralogist*, 67, 298–310.
- Pollak, H., and Bruyneel, W. (1974) Saut d'électrons et le rapport Fe²⁺/Fe³⁺ dans deux silicates. *Journal de Physique, Colloque*, 66, 35, 571–574.
- Pollak, H., DeCoster, M., and Amelinckx, S. (1962) Mössbauer effect in biotite. *Physica Status Solidi*, 2, 1653–1659.
- Pof'shin, E.V., Matyash, I.V., Tepikin, V.E., and Ivanitskii, V.P. (1972) Mössbauer effect on Fe⁵⁷ nuclei in biotite. *Soviet Physics. Crystallography*, 17, 278–280.
- Rice, C.M., and Williams, J.M. (1969) A Mössbauer study of biotite weathering. *Mineralogical Magazine*, 37, 210–215.
- Robbins, D.W., and Strens, R.G.J. (1972) Charge-transfer in ferromagnesian silicates: The polarized electronic spectra of trioctahedral micas. *Mineralogical Magazine*, 38, 551–563.
- Sanz, J., Meyers, J., Vielvoye, L., and Stone, W.E.E. (1978) The location and content of iron in natural biotites and phlogopites: A comparison of several methods. *Clay Minerals*, 13, 45–52.
- Shannon, R.D. (1976) Revised effective ionic radii and systematic studies of interatomic distances in halide and chalcogenides. *Acta Crystallographica*, A32, 751–767.
- Shinno, I., and Suwa, K. (1981) Mössbauer spectrum and polype of phlogopite with reverse pleochroism. *Preliminary Reports on African Studies (Nagoya University)*, 6, 151–157.
- Smith, G. (1978) Evidence for absorption by exchange-coupled Fe²⁺-Fe³⁺ pairs in the near infrared spectra of minerals. *Physics and Chemistry of Minerals*, 3, 375–383.
- Smith, G., Howes, B., and Hazen, Z. (1980) Mössbauer and optical spectra of biotite: A case for Fe²⁺-Fe³⁺ interactions. *Physica Status Solidi (a)*, 57, K187–K192.
- Taylor, G.L., Ruotsala, A.P., and Keeling, R.O. (1968) Analysis of iron in layer silicates by Mössbauer spectroscopy. *Clays and Clay Minerals*, 16, 381–391.
- Tricker, M.J., Winterbottom, A.P., and Freeman, A.G. (1976) Iron-57 conversion-electron Mössbauer spectroscopic study of the initial stages of the oxidation of biotite. *Journal of the Chemical Society, Dalton Transaction*, 1289–1292.
- Tripathi, R.P., and Lokanathan, S. (1978) Mössbauer study of Mg and Mn-rich amphiboles and micas. *Indian Journal of Pure and Applied Physics*, 16, 888–892.
- (1982) Mössbauer study of layered silicates minerals of Indian origin. *Indian Journal of Pure and Applied Physics*, 20, 346–352.
- Tripathi, R.P., Chandra, U., Chandra, R., and Lokanathan, S. (1978) A Mössbauer study of the effects of heating biotite, phlogopite, and vermiculite. *Journal of Inorganic and Nuclear Chemistry*, 40, 1293–1298.
- Vertes, A., Jonas, K., Czako-Nagy, I., and Nemezc, E. (1981) A

combined application of Mössbauer spectroscopy and chemical transformation for chemical analysis. *Radiochemical and Radioanalytical Letters*, 48, 93–100.

Voitovsky, Y.B., Gendler, T.S., Dainyak, L.G., and Kuzmin, R.N. (1975) Phase transformations under oxidation and decomposition of biotite. *International Conference on Mössbauer Spectroscopy Proceedings*, 1, 387–388.

Weiss, Z., Rieder, M., Chmielova, M., and Krajicek, J. (1985) Geometry of the octahedral coordination in micas: A review of refined structures. *American Mineralogist*, 70, 747–757.

Whipple, E.R. (1974) Quantitative Mössbauer spectra and chemistry of iron. Ph.D. thesis, Massachusetts Institute of Technology, Cambridge.

Yassoglov, N.J., Nobeli, C., Kostikas, A.J., and Simopoulos, A.C. (1972) Weathering of mica flakes in two soils in northern Greece evaluated by Mössbauer and conventional techniques. *Soil Science Society of America, Proceedings*, 36, 520–527.

MANUSCRIPT RECEIVED JULY 29, 1985

MANUSCRIPT ACCEPTED SEPTEMBER 2, 1986

Appendix Table 1. References used in plots and tables

1	Voitovsky et al., 1975	88	Huggins, 1976
2–3	Shinno and Suwa, 1981	89	Marfunin et al., 1971
4	Levillain et al., 1977	90–92	Tripathi and Lokanathan, 1978
5	Ivanitskiy et al., 1977	93–96	Taylor et al., 1968
6–7	Ishida and Hirowatari, 1980	97–102	Amirkhanov et al., 1980
8	Goncharov et al., 1971	103–104	Tripathi et al., 1978
9	Bagin et al., 1980	105	Goodman and Wilson, 1973
10	Annersten, 1975	106–108	Haggstrom et al., 1969b
11–13	Bowen et al., 1969	109	Yassoglov et al., 1972
14–20	Bancroft and Brown, 1975*	110	Tricker et al., 1976
21	Rice and Williams, 1969	111	Bancroft et al., 1977
22–23	Haggstrom et al., 1969a	112	Chandra and Lokanathan, 1982
24–25	Ivanitskiy et al., 1975a	113	Chandra and Lokanathan, 1977
25–33	Sanz et al., 1978	114–115	Drago et al., 1977
34–35	Ivanitskiy et al., 1975b	116–117	Ericsson et al., 1977
36–41	Annersten, 1974	118–119	Gendler et al., 1978
42	Smith et al., 1980**	120	Ivanitskiy et al., 1975c
43–45	Hogg and Meads, 1970	121	Ivanitskiy et al., 1978
46	Hogg and Meads, 1975	122	Kohn and Kakitani, 1972
47–53	Manapov and Sitdikov, 1974	127	Lefelhocz et al., 1967
54–58	Hogarth et al., 1970	128–129	Manapov and Krinari, 1976
59–63	Annersten and Olesch, 1978	130–132	Pollak et al., 1962
64–71	Levillain et al., 1981	133	Pollak and Bruyneel, 1974
72–84	Dyar, unpublished data	134–144	Pol'shin et al., 1972
85	Astakhov et al., 1975	145	Vertes et al., 1981
86	Herzenberg et al., 1968	146–151	Tripathi and Lokanathan, 1982
87	Annersten et al., 1971		

* Analyses from Dodge et al., 1969.

** Analyses from Smith, 1978.

Appendix Table 2. Sample origins

4	Massif Central Français
8	metasomatic (ore deposit)
14	monzonite, Sierra Nevada batholith
15–20	granodiorites, Sierra Nevada batholith
21	Bosahan quarry, Falmouth, England
34–35	adjacent to uranium ore
36	high amphibolite facies, gneiss SW Greenland
37	low amphibolite facies, gneiss SW Greenland
38	Revsund granite, Sweden
39	charnockite (granulite facies) Varberg, Sweden
40	metamorphosed iron formation, Sweden
41	titano-ferrous metadiabase, Nordingrd, Sweden
43–46	granites, SW England
47	granulite facies, 2 px-plag mesocratic schist
48	granulite facies, gn-hypersthene gneiss with gn-bi-sill bands
49	granulite facies, silicified gn-bi-sil gn
50	granulite facies, garnet-biotite plagiogneiss
51	amphibolite facies, gn-bi-hb metadiorite
52	amphibolite facies, gn-bi gneiss
53	amphibolite facies, biotite plagiogranite
54–55	intrusive carbonates, Gatineau region, Quebec
56–58	phlogopite-calcite, px vein dikes
59	clintonite with fassaite, grossularite, spinel, perovskite
60	clintonite with fassaite, grossularite, calcite, clinocllore, magnetite
61	clintonite with fassaite, pargasite, chondrodite, calcite, spinel, graphite
62	clintonite with fassaite, calcite, monticellite: contact marble
72	monzonite, Sierra Nevada batholith (same as 15)
73	granodiorite, Sierra Nevada batholith (same as 16)
74	granodiorite, Sierra Nevada batholith (same as 17)
75	granodiorite, Sierra Nevada batholith (same as 18)
76	Pikes Peak granite
77	Lost Creek, Montana granite
78	Cape Ann granite
79	banded iron formation, with riebeckite, hem, mag, qtz, ank, stil
80	banded iron formation, hematite, riebeckite, low grade
81	banded iron formation, "higher grade"
83–84	garnet, sillimanite, muscovite, quartz, plagioclase, rutile
94, 96	banded iron formation, Marquette Iron Range
111	granodiorite, Nova Scotia
118–119	pegmatites of Ukrainian shield

Appendix Table 3. Compositions and Mössbauer data

Sample #	1B	2P	3P	4L	5B	6P	7P	8S	9B	10B	11B	12B	13P	14B	15B	16B	17B	18B	19B	20B	21B
Si ⁴⁺	5.50	5.89	5.99	7.00	5.14	5.40	6.20	6.00	5.34	4.50	5.10	4.96	5.12	5.60	5.53	5.42	5.37	5.63	5.52	5.62	5.29
Al ³⁺	2.04	1.76	1.68	0.98	2.86	2.20	1.40	2.00	2.10	3.50	2.90	3.04	2.88	2.40	2.47	2.58	2.63	2.37	2.48	2.38	2.22
Fe ³⁺	0.46	0.32	0.28	0.02	-	0.20	0.40	-	0.56	-	-	-	-	-	-	-	-	-	-	-	0.49
Sum Tet	8.00	7.97	7.95	8.00	8.00	8.00	8.00	8.00	8.00	8.00	8.00	8.00	8.00	8.00	8.00	8.00	8.00	8.00	8.00	8.00	8.00
Al	1.28	-	-	2.44	0.62	-	-	4.80	1.04	3.00	0.96	1.34	0.90	0.42	0.24	0.67	0.76	0.36	0.48	0.42	1.56
Ti	0.22	0.01	0.03	-	0.24	-	-	0.60	0.20	-	0.28	0.10	0.14	0.29	0.29	0.35	0.36	0.19	0.18	0.32	0.28
Fe ³⁺	0.00	-	-	0.00	0.34	0.20	-	-	0.00	0.16	0.28	0.48	0.16	0.42	0.48	0.44	0.17	0.39	0.49	0.42	0.00
Mg	2.10	5.52	5.49	0.02	1.90	3.40	5.00	-	2.02	-	1.78	0.48	4.04	2.45	2.64	1.22	1.56	2.73	2.53	2.17	1.15
Fe ²⁺	2.36	0.48	0.39	0.42	2.60	-	0.40	0.60	2.16	4.34	2.22	2.90	0.58	2.12	2.02	2.78	2.74	1.89	1.97	2.38	2.34
Mn	0.04	0.01	-	0.05	0.02	2.00	0.60	-	0.02	-	-	-	-	0.05	0.05	0.14	0.06	0.05	0.11	0.04	0.03
Li	0.00	-	-	1.50	-	-	-	-	-	-	-	-	-	-	-	-	-	-	-	-	-
Other	-	-	Cr 0.01	-	-	Ba 0.20	-	-	-	-	-	-	-	-	-	-	-	-	-	-	-
Sum Oct	6.00	6.02	5.92	6.00	5.72	5.80	6.00	6.00	5.44	6.00	5.52	5.30	5.82	5.75	5.72	5.60	5.65	5.61	5.76	5.75	5.36
Ca	0.10	0.02	0.01	-	0.12	-	-	-	0.10	-	-	-	-	0.03	0.09	0.00	0.00	0.10	0.09	0.09	0.00
Na	0.10	0.10	0.01	0.10	0.22	0.40	-	-	0.10	-	0.08	0.06	0.12	0.07	0.06	0.15	0.13	0.07	0.09	0.08	0.10
K	1.90	1.90	2.01	1.74	1.54	1.60	1.80	2.40	1.80	2.00	1.70	1.80	1.62	1.84	1.63	1.86	1.85	1.63	1.61	1.77	1.76
Other	-	-	-	Rb 0.16	-	-	-	-	-	-	-	-	-	-	-	-	-	-	-	-	-
Sum A	2.10	2.02	2.03	2.00	1.88	2.00	1.80	2.40	2.00	2.00	1.78	1.86	1.74	1.94	1.73	2.01	1.98	1.80	1.79	1.94	1.86
δ1	1.19	1.12	1.12	1.16	1.20	-	1.13	1.17	1.19	1.13	1.11	1.12	1.11	1.12	1.13	1.13	1.14	1.13	1.12	1.13	1.14
δ1	2.62	2.65	2.65	2.62	2.86	-	2.52	2.52	2.58	2.54	2.47	2.51	2.44	2.62	2.62	2.57	2.62	2.65	2.61	2.61	2.56
δ2	1.17	-	-	1.18	1.17	-	-	-	1.19	1.18	-	-	-	1.10	1.10	1.11	1.13	1.09	1.09	1.11	1.15
δ2	2.24	-	-	2.99	2.29	-	-	-	2.13	2.00	-	-	-	2.13	2.15	2.06	2.15	2.20	2.17	2.14	2.63
δ3	-	-	-	-	0.43	0.34	-	-	-	0.40	-	-	-	0.46	0.47	0.48	-	0.49	0.49	0.51	-
δ3	-	-	-	-	1.12	1.02	-	-	-	0.76	-	-	-	1.00	1.05	1.00	-	1.03	1.00	1.05	-
δ4	-	-	-	-	0.46	-	-	-	-	-	0.54	0.54	0.44	0.45	0.49	0.52	0.60	0.49	0.48	0.51	-
δ4	-	-	-	-	0.62	-	-	-	-	-	0.60	0.80	0.90	0.42	0.50	0.47	0.57	0.52	0.52	0.51	-
δ5	0.20	0.20	0.24	0.25	-	0.26	0.15	-	0.14	-	-	-	-	-	-	-	-	-	-	-	-0.03
δ5	1.23	0.52	0.47	0.35	-	0.62	0.63	-	1.23	-	-	-	-	-	-	-	-	-	-	-	0.24
Fe ²⁺ /ΣFe	0.84	0.50	0.58	0.96	0.88	0.20	0.50	1.00	0.79	0.95	0.89	0.86	0.78	0.83	0.81	0.86	0.94	0.83	0.81	0.85	0.17
M2/M1 Fe ²⁺	-	-	-	1.91	2.14	-	-	-	-	-	-	-	-	-	-	-	-	-	-	-	-

Sample #	22B	23A	24B	25B	26P	27P	28P	29B	30B	31B	32B	33B	34B	35B	36B	37B	38B	39B	40B	41B	42B
Si ⁴⁺	5.63	6.00	5.60	5.60	6.18	6.08	5.68	5.42	5.48	5.48	6.00	6.00	5.28	5.59	5.25	5.39	5.50	5.45	5.92	5.20	5.44
Al ³⁺	2.37	2.00	2.40	2.40	1.82	1.92	2.32	2.58	2.52	2.52	2.00	1.76	2.73	2.41	2.75	2.61	2.50	2.35	2.05	2.33	2.56
Fe ³⁺	-	-	-	-	-	-	-	-	-	-	-	0.24	-	-	-	-	-	-	0.20	0.03	0.47
other	-	-	-	-	-	-	-	-	-	-	-	-	-	-	-	-	-	-	-	-	-
Sum Tet	8.00	8.00	8.00	8.00	8.00	8.00	8.00	8.00	8.00	8.00	8.00	8.00	8.01	8.00	8.00	8.00	8.00	8.00	8.00	8.00	8.00
Al	0.02	2.00	0.62	1.60	0.18	0.08	0.18	0.50	1.20	0.36	0.12	-	-	0.86	0.33	0.36	0.18	0.00	0.00	0.00	0.88
Ti	0.46	-	0.21	-	0.34	0.26	0.26	0.34	0.26	0.10	0.04	0.12	0.10	0.25	0.37	0.23	0.40	0.67	0.12	0.65	0.16
Fe ³⁺	0.75	1.95	0.41	0.60	0.04	0.09	0.18	0.09	0.34	0.02	0.03	0.06	1.52	0.46	0.32	0.50	1.21	0.38	0.13	2.06	0.73
Mg	0.48	-	2.07	1.60	3.80	3.20	2.04	2.16	0.92	5.10	5.46	5.36	3.73	1.61	2.39	2.30	0.46	2.27	4.30	0.52	2.34
Fe ²⁺	3.97	4.05	2.48	2.00	1.50	2.08	2.88	2.52	2.48	0.32	0.34	0.32	0.27	2.04	1.94	2.11	2.95	2.31	1.27	3.36	1.54
Mn	0.05	-	-	-	0.02	0.10	0.08	0.06	0.08	-	0.02	-	0.02	0.02	0.02	0.02	0.05	0.01	0.05	0.03	0.08
Li	-	-	-	-	0.18	0.10	0.08	0.04	0.38	0.01	0.03	-	-	-	-	-	-	-	-	-	-
Other	-	-	-	-	-	-	-	-	-	-	-	-	-	-	-	-	-	-	-	-	-
Sum Oct	5.73	6.00	5.78	5.80	6.06	5.91	5.70	5.71	5.66	5.91	6.04	5.86	5.64	5.24	5.37	5.52	5.25	5.64	5.87	6.62	5.73
Ca	-	-	0.20	-	0.16	0.02	0.04	0.04	0.03	0.10	0.06	0.02	0.04	-	-	-	-	-	-	-	0.00
Na	-	-	-	0.20	0.14	0.18	0.12	0.06	0.10	0.12	0.08	0.02	0.08	0.17	-	-	-	-	-	-	-
K	1.88	2.00	1.80	1.80	1.88	1.88	1.96	1.86	1.88	1.70	1.90	1.90	1.74	-	-	-	-	-	-	-	-
Other	-	-	-	-	-	-	-	-	-	-	-	-	-	-	-	-	-	-	-	-	-
Sum A	1.88	2.00	2.00	2.00	2.18	2.08	2.12	1.96	2.01	1.92	2.04	1.94	1.86	1.99	1.78	1.76	1.92	1.90	1.84	1.60	1.89
δ1	1.13	1.15	1.14	1.15	1.14	1.15	1.14	1.15	1.13	1.12	1.12	1.13	1.19	1.18	1.06	1.07	1.06	1.06	1.05	1.05	1.04
δ1	2.56	2.56	2.61	2.66	2.61	2.60	2.60	2.66	2.59	2.56	2.60	2.65	2.66	2.66	2.56	2.62	2.60	2.56	2.58	2.57	2.60
δ2	1.11	1.11	1.13	1.14	1.12	1.10	1.10	1.12	1.12	1.12	1.13	-	1.18	1.18	1.03	1.05	1.01	1.02	1.03	1.05	1.01
δ2	2.17	2.18	2.10	2.29	2.20	2.16	2.17	2.23	2.17	2.22	2.20	-	2.28	2.18	2.10	2.19	2.20	2.13	2.21	2.12	2.23
δ3	0.55	0.54	0.46	0.46	0.54	0.57	0.50	0.51	0.49	0.61	0.61	-	0.54	0.50	0.41	0.50	0.43	0.41	0.51	0.50	0.48
δ3	0.55	0.52	0.85	1.00	0.60	0.56	0.69	0.65	0.60	0.98	0.97	-	0.76	1.11	1.02	0.72	0.93	0.74	1.17	0.88	0.78
δ4	-	-	-	-	-	-	-	-	-	-	-	-	-	0.52	0.43	0.52	0.40	0.39	0.46	0.54	0.46
δ4	-	-	-	-	-	-	-	-	-	-	-	-	-	0.64	0.50	0.57	0.50	0.57	0.65	0.34	0.32
δ5	-	-	-	-	-	-	-	-	-	-	0.26	-	-	-	-	-	-	-	-	-	-
δ5	-	-	-	-	-	-	-	-	-	-	0.45	-	-	-	-	-	-	-	-	-	-
Fe ²⁺ /ΣFe	0.84	0.68	0.86	0.78	0.90	0.95	0.82	0.89	0.96	0.88											

Appendix Table 3.—Continued

Sample #	43P	44B	45Z	46B	47B	48B	49B	50B	51B	52B	53B	54P	55P	56P	57P	58P	59C	60C	61C	62C	63C
Si ⁴⁺	5.60	5.30	6.92	5.88	5.51	5.35	5.25	5.11	5.14	5.23	5.38	5.96	6.10	5.65	5.69	5.61	2.41	2.41	2.73	2.35	2.23
Al ³⁺	2.40	2.70	1.08	2.12	2.49	2.47	2.56	2.89	2.77	2.77	2.62	1.69	1.83	2.08	2.30	2.38	5.49	5.47	5.27	5.38	5.25
Fe ³⁺	-	-	-	-	-	0.18	0.20	-	0.09	-	-	0.29	0.07	0.27	0.01	0.01	0.10	0.12	-	0.27	0.52
Sum Tet	8.00	8.00	8.00	8.00	8.00	8.00	8.00	8.00	8.00	8.00	8.00	7.94	8.00	8.00	8.00	8.00	8.00	8.00	8.00	8.00	8.00
Al	0.16	0.39	2.31	1.81	0.11	0.52	1.09	0.68	0.00	0.55	0.30	0.00	0.00	0.00	0.00	0.00	1.44	1.53	1.13	1.70	1.40
Ti	0.23	0.38	0.03	0.04	0.48	0.47	0.18	0.23	0.44	0.27	0.27	0.02	0.02	0.12	0.15	0.13	-	-	-	-	-
Fe ³⁺	0.03	0.54	0.09	0.24	0.21	0.05	0.19	0.35	0.54	0.40	0.33	0.00	0.05	0.22	0.16	0.14	0.00	0.03	0.00	0.03	0.08
Mg	5.07	2.18	0.04	0.11	2.70	3.22	2.01	2.15	1.94	2.37	2.61	5.59	5.13	5.19	4.25	5.31	4.42	4.39	4.80	4.20	4.45
Fe ²⁺	0.37	2.05	0.66	2.14	2.18	1.41	2.17	2.30	2.76	2.13	2.16	0.49	0.69	0.16	1.04	0.15	0.10	0.07	0.17	0.05	0.00
Mn	0.00	0.00	0.68	0.04	0.02	0.00	0.01	0.04	0.03	0.01	0.04	0.01	0.00	0.01	0.01	0.00	-	-	-	-	-
Li	-	-	2.29	0.91	-	-	-	-	-	-	-	-	-	-	-	-	-	-	-	-	-
Other	-	-	-	-	-	-	-	-	-	-	-	-	-	-	-	-	-	-	-	-	-
Sum Oct	5.86	5.54	6.10	5.29	5.70	5.67	5.65	5.75	5.71	5.73	5.71	6.11	5.89	5.70	5.61	5.73	5.96	6.02	6.10	5.98	5.93
Ca	0.07	0.19	0.02	0.21	0.05	0.07	0.03	0.03	0.20	0.03	0.09	0.03	0.01	0.00	0.00	0.00	1.99	1.98	1.96	1.97	2.23
Na	0.36	0.14	0.07	0.10	0.02	0.01	0.08	0.05	0.03	0.02	0.04	0.13	0.13	0.67	0.86	0.63	0.24	0.00	0.02	0.00	0.00
K	1.55	1.46	1.83	1.80	1.69	1.64	1.66	1.76	1.58	1.78	1.83	1.80	1.88	1.82	1.78	1.89	0.02	0.00	0.00	0.00	0.00
Other	-	-	-	-	-	-	-	-	-	-	-	-	-	-	-	-	-	-	-	-	-
Sum A	1.98	1.79	1.92	2.21	1.76	1.72	1.77	1.84	1.81	1.83	1.96	1.96	2.02	2.49	2.64	2.52	2.25	1.98	1.98	1.97	2.23
δ1	1.10	1.07	1.15	1.13	1.13	1.13	1.15	1.15	1.13	1.13	1.14	1.18	1.19	1.14	1.17	1.15	1.08	-	1.13	1.08	-
Δ1	2.56	2.58	2.65	2.44	2.57	2.44	2.65	2.62	2.57	2.65	2.61	2.76	2.76	2.62	2.79	2.76	2.48	-	2.46	2.39	-
δ2	1.08	1.06	-	1.13	1.09	1.10	1.13	1.14	1.12	1.10	1.11	1.28	1.29	1.24	1.28	1.14	1.04	1.09	1.15	-	-
Δ2	2.24	2.14	-	2.74	2.19	2.07	2.18	2.19	2.17	2.22	2.21	2.97	2.95	2.82	3.01	2.97	1.72	2.11	1.85	-	-
δ3	0.47	0.39	0.40	0.38	0.63	0.59	0.63	0.60	0.63	0.60	0.60	-	0.64	0.53	0.54	0.50	0.52	-	-	-	0.49
Δ3	0.80	0.72	0.89	0.83	0.64	0.57	0.64	0.57	0.78	0.57	-	-	1.22	0.94	1.15	1.06	1.05	1.20	-	-	1.08
δ4	-	-	-	-	0.38	-	-	-	-	-	-	0.35	-	-	-	-	-	-	-	-	-
Δ4	-	-	-	-	0.57	-	-	-	-	-	0.50	-	-	-	-	-	-	-	-	-	-
δ5	-	-	-	-	-	0.06	0.13	-	0.10	-	-	0.19	0.21	-	-	-	0.27	0.24	-	0.26	0.24
Δ5	-	-	-	-	0.50	0.36	-	-	0.43	-	-	0.44	0.44	-	-	-	0.62	0.68	-	0.65	0.80
Fe ²⁺ /ΣFe	0.90	0.81	0.83	0.89	0.80	0.84	0.85	0.83	0.82	0.83	0.80	0.74	0.86	0.82	0.94	0.81	0.35	0.26	1.00	0.24	-
M2/M1 Fe ²⁺	1.65	1.24	-	3.50	1.20	2.19	1.93	1.54	2.15	2.04	1.96	-	-	-	-	-	4.63	-	3.23	-	-

Sample #	64L	65Z	66Z	67Z	68S	69S	70S	71S	72B	73B	74B	75B	76B	77B	78A	79A	80A	81A	82P	83B	84B
Si ⁴⁺	7.40	5.68	5.39	5.67	4.98	5.14	5.19	3.99	5.47	5.49	5.61	5.49	5.56	5.85	5.49	6.06	6.51	5.85	5.94	5.27	5.36
Al ³⁺	0.60	2.32	2.61	2.33	3.02	2.86	2.81	4.01	2.53	2.51	2.39	2.51	2.29	1.84	2.15	1.94	0.18	1.05	1.59	2.73	2.64
Fe ³⁺	-	-	-	-	-	-	-	-	-	-	-	-	0.15	0.30	0.36	0.85	1.31	1.10	0.47	-	-
Sum Tet	8.00	8.00	8.00	8.00	8.00	8.00	8.00	8.00	8.00	8.00	8.00	8.00	8.00	8.00	8.00	8.00	8.00	8.00	8.00	8.00	8.00
Al	2.13	2.42	2.35	2.29	2.16	2.24	2.18	1.84	0.40	0.23	0.34	0.18	0.00	1.88	0.00	0.00	0.00	0.00	0.00	0.81	0.80
Ti	-	-	-	-	-	-	-	-	0.18	0.32	0.19	0.29	0.30	0.07	0.43	0.00	0.00	0.02	0.01	0.16	0.16
Fe ³⁺	0.00	0.00	0.18	0.33	0.03	0.16	0.26	0.21	0.66	0.57	0.62	0.65	0.60	0.30	0.25	0.30	0.17	0.24	0.30	0.37	0.26
Mg	-	-	-	-	-	-	-	-	2.51	2.12	2.72	2.62	0.22	0.01	0.07	2.70	1.51	0.77	5.11	2.14	2.15
Fe ²⁺	0.45	1.58	1.45	1.25	2.55	2.18	2.13	3.96	1.78	2.16	1.66	1.84	4.39	2.40	2.16	2.96	4.22	4.77	0.47	2.30	2.36
Mn	-	-	-	-	-	-	-	-	0.11	0.04	0.05	0.05	0.09	0.22	0.06	0.00	0.00	0.01	0.00	0.00	0.01
Li	3.53	2.09	2.09	2.04	1.30	1.31	1.25	0.00	-	-	-	-	-	-	-	-	-	-	-	-	-
Other	-	-	-	-	-	-	-	-	-	-	-	-	-	-	-	-	-	-	-	-	-
Sum Oct	6.11	6.09	6.07	5.91	6.04	5.89	5.82	6.01	5.64	5.44	5.58	5.63	5.60	4.88	4.97	5.96	5.90	5.80	5.90	5.78	5.74
Ca	0.00	0.00	0.00	0.00	0.00	0.00	0.00	0.00	0.09	0.09	0.10	0.09	0.01	0.00	0.00	0.00	0.07	0.12	0.00	0.00	0.00
Na	0.00	0.00	0.00	0.00	0.00	0.00	0.00	0.00	0.09	0.07	0.07	0.06	0.03	0.05	0.03	0.05	0.00	0.00	0.03	0.10	0.08
K	1.78	1.81	2.02	1.90	2.05	2.02	1.97	1.96	1.59	1.92	1.63	1.62	1.87	1.97	1.66	1.67	1.40	2.06	1.91	1.56	1.69
Other	-	-	-	-	-	-	-	-	-	-	-	-	-	-	-	-	-	-	-	-	-
Sum A	1.78	1.81	2.02	1.90	2.05	2.02	1.97	1.96	1.77	2.08	1.80	1.77	1.91	2.02	1.69	1.72	1.47	2.18	1.94	1.66	1.77
δ1	1.17	1.13	1.17	1.14	1.16	1.17	1.13	1.14	1.13	1.13	1.13	1.12	1.13	1.14	1.12	1.13	1.13	1.10	1.12	1.14	1.14
Δ1	2.63	2.42	2.57	2.66	2.36	2.51	2.64	2.55	2.60	2.57	2.60	2.58	2.53	2.68	2.50	2.67	2.60	2.55	2.63	2.63	2.61
δ2	1.18	1.13	1.18	1.15	1.15	1.17	1.14	-	1.07	1.10	1.07	1.09	1.10	1.10	1.15	1.12	1.15	1.16	-	1.13	1.14
Δ2	2.96	2.77	2.90	2.93	2.69	2.83	2.90	-	2.22	2.12	2.15	2.15	2.06	2.36	1.90	2.82	2.83	2.16	-	2.19	2.15
δ3	-	-	0.40	0.42	-	0.38	0.48	0.34	0.42	0.39	0.41	0.45	0.43	0.34	0.42	0.39	0.36	0.42	-	0.43	0.43
Δ3	-	-	0.61	0.88	-	0.69	0.98	0.39	1.24	1.16	1.16	1.17	0.99	0.74	0.98	0.94	0.56	1.01	-	1.19	1.20
δ4	-	-	-	0.38	-	-	0.35	-	0.41	0.44	0.39	0.46	0.39	-	0.37	0.42	-	-	-	0.44	0.44
Δ4	-	-	-	0.54	-	-	0.52	-	0.55	0.47	0.52	0.52	0.31	-	0.61	0.46	-	-	-	0.28	0.37
δ5	-	-	-	-	-	-	-	-	-	-	-	-	-	0.11	0.20	0.19	0.21	0.20	0.19	-	-
Δ5	-	-	-	-	-	-	-	-	-	-	-	-	-	0.15	0.37	0.39	0.40	0.45			

Appendix Table 4. Data from papers with no compositional information

Sample #	85L	86Z	87P	88P	89P	90P	91P	92P	93L	94B	95B	96B	97B	98B	99B	100B	101B	102B	103B	104B	105B	106B	107B	
61	1.06	1.08	-	1.00	1.41	1.02	1.09	1.09	1.11	1.16	1.14	1.11	1.10	1.11	1.19	1.12	1.12	1.19	1.12	1.11	1.13	1.15	1.12	
Δ1	2.73	3.13	-	2.62	2.70	2.42	2.56	2.56	2.40	2.60	2.45	2.50	2.66	2.64	2.60	2.62	2.66	2.67	2.42	2.54	2.64	2.48	2.48	
Δ2	1.06	-	-	-	1.15	-	1.05	0.96	-	-	-	-	1.10	1.10	1.18	1.14	1.09	1.17	-	1.10	1.11	-	-	
Δ3	2.38	-	-	-	2.20	-	2.17	2.21	-	-	-	2.21	2.21	2.32	2.25	2.36	2.29	-	-	2.07	2.19	-	-	
Δ4	-	-	-	-	0.31	0.35	-	0.48	-	-	0.39	0.39	-	-	-	0.58	-	-	-	0.45	0.43	0.38	0.46	
Δ5	-	-	-	-	0.36	0.87	-	1.11	-	-	0.95	0.95	-	-	-	0.80	-	-	-	0.86	1.14	0.89	1.16	
Fe ²⁺ /ΣFe	-	-	-	-	-	0.17	0.76	0.26	-	-	-	-	-	-	-	-	-	-	-	-	0.82	0.57	0.81	0.74
M2/M1 Fe ²⁺	-	-	-	-	-	-	1.92	2.25	-	-	-	-	-	-	-	-	-	-	-	-	3.56	1.71	-	-
		108B	109B	110B	111B	112B	113B	114B	115B	116B	117B	118B	119B	120B	121B	122G	123B	124B	125B	126B	127B	128B	129B	130B
61	1.18	-	1.11	1.11	1.11	1.04	1.08	1.12	1.11	1.12	1.13	1.19	1.11	1.13	1.09	1.12	1.15	1.21	1.25	1.10	1.13	1.14	1.27	
Δ1	2.48	-	2.58	2.53	2.54	2.59	2.63	2.43	2.58	2.56	2.62	2.58	2.67	2.60	2.34	2.33	2.40	2.57	2.53	2.50	2.57	2.61	2.71	
Δ2	-	1.04	1.08	1.08	1.10	1.03	1.07	-	1.08	1.10	1.11	1.19	1.12	1.09	-	-	-	-	-	-	-	1.12	1.13	1.08
Δ3	-	2.02	2.15	1.98	2.07	2.09	2.22	-	2.24	2.09	2.24	2.13	2.10	2.23	-	-	-	-	-	-	-	2.17	2.21	2.32
Δ4	-	0.43	0.43	0.51	0.43	0.34	-	-	0.57	0.60	-	-	0.42	-	-	0.36	0.37	0.36	0.37	-	0.63	-	-	
Δ5	-	0.91	0.71	0.17	1.13	1.70	-	-	0.71	0.71	-	-	1.81	-	-	0.70	0.72	0.70	0.71	-	0.78	-	-	
Fe ²⁺ /ΣFe	0.82	-	0.70	0.83	0.83	-	-	-	0.91	0.89	-	-	0.86	-	-	-	-	-	-	-	-	0.82	0.80	-
M2/M1 Fe ²⁺	-	-	3.13	-	3.61	-	-	-	1.22	2.30	-	-	1.45	-	-	-	-	-	-	-	-	2.15	1.96	-
		131B	132B	133B	134B	135B	136B	137B	138B	139B	140B	141B	142B	143B	144B	145B	146B	147B	148B	149B	150B	151B		
61	1.33	1.34	1.12	1.15	1.15	1.16	1.16	1.16	1.16	1.16	1.17	1.17	1.18	1.19	1.13	1.00	1.05	1.10	1.10	1.11	1.12			
Δ1	2.81	2.87	2.66	2.61	2.68	2.67	2.70	2.70	2.65	2.67	2.60	2.70	2.80	2.64	2.56	2.65	2.57	2.54	2.54	2.58	2.51			
Δ2	1.14	1.14	1.13	1.11	1.12	1.15	1.11	1.14	1.13	1.15	1.11	1.14	1.17	1.14	1.01	1.00	1.02	1.10	1.08	1.13	1.07			
Δ3	2.41	2.47	2.20	2.16	2.22	2.22	2.26	2.24	2.16	2.22	2.16	2.23	2.40	2.20	2.20	2.01	2.24	2.07	2.16	2.02	2.23			
Δ4	-	-	0.40	-	-	-	-	-	-	-	-	-	-	-	-	0.48	0.43	0.43	0.34	-	0.34			
Δ5	-	-	0.96	-	-	-	-	-	-	-	-	-	-	-	-	0.61	1.14	1.14	1.02	-	1.13			
Fe ²⁺ /ΣFe	-	-	-	-	-	-	-	-	-	-	-	-	-	-	-	-	0.48	0.44	0.44	0.46	-	0.46		
M2/M1 Fe ²⁺	-	-	0.13	-	-	-	-	-	-	-	-	-	-	-	-	0.32	0.48	0.48	0.51	-	0.52			
Δ5	-	-	0.54	-	-	-	-	-	-	-	-	-	-	-	0.58	-	-	-	-	-	-			
Fe ²⁺ /ΣFe	-	-	-	-	-	-	-	-	-	-	-	-	-	-	-	0.38	0.46	0.83	0.75	1.00	0.53			
M2/M1 Fe ²⁺	-	-	-	-	-	-	-	-	-	-	-	-	-	-	-	2.45	2.54	3.61	2.41	3.16	2.79			